Ultra-fast HPM Detectors Improve NAD(P)H FLIM

Wolfgang Becker, Lukas Braun, Becker & Hickl GmbH

Abstract: Metabolic imaging by NAD(P)H FLIM requires the decay functions in the individual pixels to be resolved into the decay components of bound and unbound NAD(P)H. Metabolic information is contained in the lifetime and relative amplitudes of the components. The separation of the decay components and the accuracy of the amplitudes and lifetimes improves substantially by using the ultra-fast HPM-100-06 and HPM-100-07 hybrid detectors. The IRF width in combination with the SPC-150N and SPC-150NX TCSPC modules is less than 20 ps [1]. An IRF this fast does not interfere with the fluorescence decay. The usual deconvolution process in the data analysis then virtually becomes a simple curve fitting, and the decay parameters are obtained at unprecedented accuracy.

Metabolic Imaging

NADH and its phosphorylated form, NADPH, are natural coenzymes that are involved in the energy production of the cell. The reduced forms of NADH and NADPH are fluorescent. It is known that the fluorescence lifetimes depend on the binding to proteins [13, 16]. The bound-NADH lifetime is in the range of 1.2 ns to 4 ns, the unbound-NADH lifetime in the range from about 300 ps to 500 ps. For NADPH the situation is similar, with slightly different lifetimes of the components [6]. The concentration ratio of bound and unbound NADH depends on the type of the metabolism: When the cell is in the state of oxidative phosphorylation the bound/unbound ratio is higher than in the state of glycolysis. Consequently, the relative amplitudes of the decay components change with the type of metabolism, and so does the mean fluorescence lifetime. Since normal cells are running preferentially oxydative phosphorylation while tumor cells are running glycolysis the corresponding changes in the fluorescence decay parameters bear the potential to distinguish between healthy cells and tumor cells [5, 15, 19, 20, 21, 24]. Changes in the NADH decay parameters are also observed during maturation of stem cells, during hypoxia, and during infection, during wound healing [3, 9, 10, 11, 12, 14, 18,]. The NADH lifetime in combination with the NADH/FAD redox ratio [8] has been used to predict drug response in breast cancer [22, 23]. Please see also [3] and [4] for a summary.

NADH FLIM with Fast Detectors

In principle, FLIM of NAD(P)H is possible with all bh FLIM systems. NAD(P)H can be excited by one-photon excitation at a wavelength of 375 nm or shorter, or by two-photon excitation in the range of 720 nm to about 780 nm. Two-photon excitation is usually preferred because it is considered less invasive to the cells (though this has never been directly proved). In any case, two photon excitation has the advantage that it penetrates much deeper into tissue, and that it has no problems with optical aberrations of the microscope optics in the UV. Another advantage of two-photon excitation is that the pulse width of the femtosecond laser does not contribute to the temporal instrument-response function (IRF) of the TCSPC FLIM system. The system therefore delivers the shortest possible IRF for a given detector-TCSPC combination. Typical IRF widths are 120 ps for GaAsP hybrid detectors, 250 ps for fast conventional PMTs, and about 300 ps for conventional PMTs with GaAsP cathodes [3]. This is not much faster than the dominating decay time of the unbound NADH, which is about 300 ps [6]. It can therefore be expected hat faster detectors improve the accuracy of the fluorescence-decay analysis of NADH FLIM. However, there is a problem. The GaAsP cathode of the typical high-efficiency FLIM detectors limits the speed to

about 120 ps. Faster detectors either have extremely small active areas (SPADS) and are thus not applicable to NDD detection in two-photon microscopes, or they have conventional photocathodes with low quantum efficiency (PMTs). A possible compromise are the new Hamamatsu R10467-06 and -07 hybrid detectors with high-efficiency bi-alkali and multi-alkali cathodes. Although the photocathodes do not reach the quantum efficiency of a GaAsP cathode the hybrid detector principle makes up for a part of the loss: Unlike a conventional PMT a hybrid detector has no loss of photoelectrons at the first dynode. Virtually all photoelectrons that leave the photocathode also cause a pulse at the output of the detector. We have shown recently that the HPM-100-06 and -07 detectors (based on the R10467-06 and -07) deliver an IRF width of less than 20 ps when operated with SPC-150N, SPC-150NX or SPC-180NX TCSPC modules [1]. An IRF this fast does not interfere with the fluorescence decay. The usual deconvolution process in the data analysis [3] then virtually becomes a simple curve fitting. It can therefore be expected that the high time resolution delivers a better photon efficiency in the data analysis and thus makes up for the lower sensitivity.

Results

For recording the data shown below we used a Zeiss LSM 880 NLO multiphoton microscope with an HPM-100-06 and an HPM-100-07 attached to the NDD output via the usual Zeiss NDD T adapter [2]. The signals were recorded by a Simple-Tau 152 system with two SPC-150N TCSPC modules. The system is able to record in two wavelength channels in parallel, the images shown here are from a wavelength channel from 440 nm to 480 nm. The excitation wavelength was 740 nm. The data were recorded with 512 x 512 pixels and 1024 time channels per pixel. The time channel width was 10 ps.

A lifetime image of the amplitude-weighted lifetime of a double-exponential fit is shown in Fig. 1, left. Decay data in a selected spot of 9x9 pixels on the right. As expected, the time resolution of the detection system is excellent. The rise of the fluorescence occurs over less than two time channels, indicating that the IRF is indeed shorter than 20 ps.

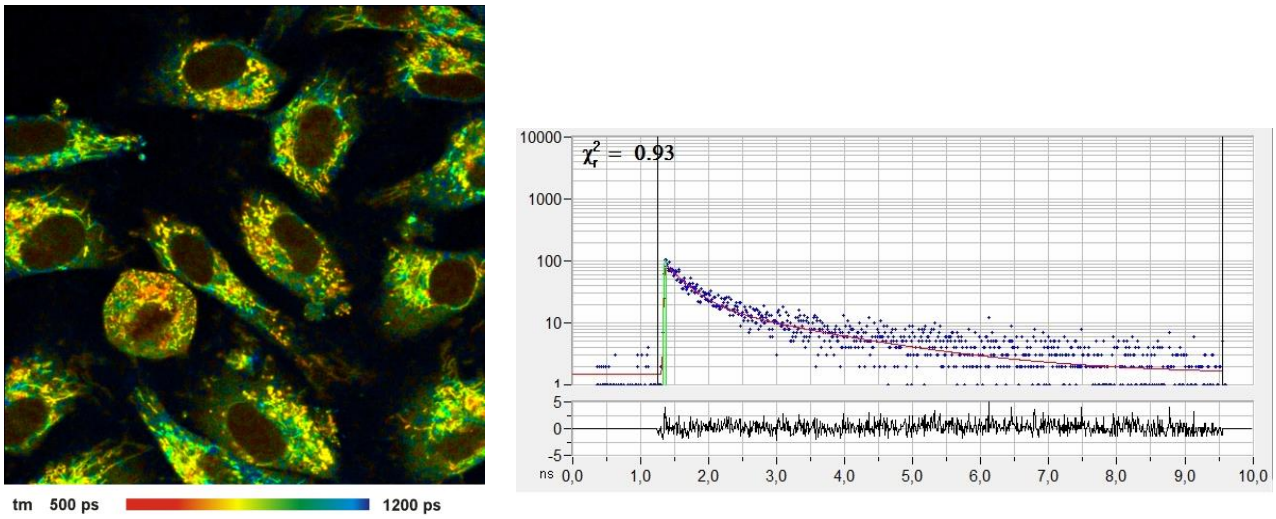

Fig. 1: Left: NADH Lifetime image, amplitude-weighted lifetime of double-exponential fit. Right: Decay curve in selected spot, 9x9 pixel area. FLIM data format 512x512 pixels, 1024 time channels. Time-channel width 10ps.

Images of the amplitude ratio, a1/a2 (unbound/bound ratio), and of the fast (t1, unbound NADH) and the slow decay component (t2, bound NADH) are shown in Fig. 2. Such images are normally

noisy, and visibly contain fitting artefacts. Not so in the data recorded with the fast detectors and SPC modules. Due to the near-ideal temporal resolution the FLIM data analysis delivers the decay components at extremely high precision, and the images are free of fitting noise and fitting artefacts.

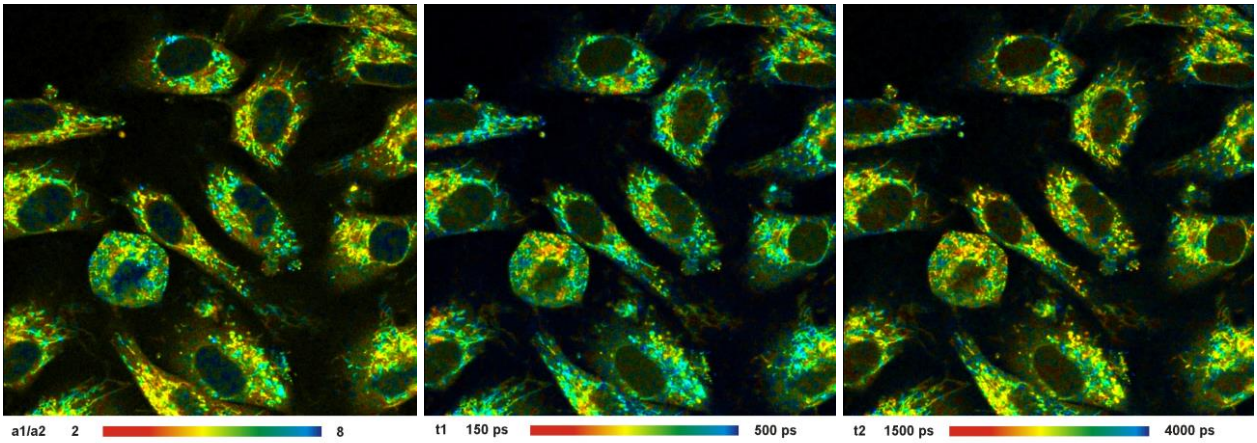

Fig. 2: Left to right: Images of the amplitude ratio, a1/a2 (unbound/bound ratio), and of the fast (t1, unbound NADH) and the slow decay component (t2, bound NADH). FLIM data format 512x512 pixels, 1024 time channels. Time-channel width 10ps.

Conclusion

The ultra-fast HPM-100-06 and HPM-100-07 hybrid detectors in combination with the SPC-150N TCSPC modules improve the accuracy of NAD(P)H FLIM dramatically. The IRF is so fast that it does no longer interfere with the decay times of the fast fluorescence components. The deconvolution process in the data analysis therefore virtually becomes a simple curve fitting, and the decay parameters are obtained at unprecedented accuracy. Even the a_1/a_2 images and the t_1 and t_2 images are virtually free of noise or fitting artefacts.

Acknowledgements

The data shown in this application note were recorded at the 2nd International Workshop on Advanced Time-Resolved Imaging Techniques at BioCev, Vestec near Prague , May 16-17, 2017. We thank Dr. Aleš Benda of BioCev for providing the LSM 880 NLO and Dr. Ondrej Šebasta of Charles University for providing his Simple Tau system and the NDD T adapter for the experiments.

References

1. Becker & Hickl GmbH, Sub-20ps IRF Width from Hybrid Detectors and MCP-PMTs. Application note, available on www.becker-hickl.com
2. Becker & Hickl GmbH , Modular FLIM Systems for ZeissLSM 710 / 780 / 880 Family Laser Scanning Microscopes. User Handbook, available on www.becker-hickl.com
3. W. Becker, The bh TCSPC handbook. Becker & Hickl GmbH, 9th ed. (2021). Available on www.becker-hickl.com
4. W. Becker (ed.) Advanced time-correlated single photon counting applications. Springer, Berlin, Heidelberg, New York (2015)

5. D.K. Bird , L. Yan , K. M. Vrotsos , K. E. Eliceiri , E. M. Vaughan. Metabolic mapping of MCF10A human breast cells via multiphoton fluorescence lifetime imaging of coenzyme NADH. Cancer Res 65:8766–8773 (2005)
6. T. S. Blacker, Z. F. Mann, J. E. Gale, M. Ziegler, A. J. Bain, G. Szabadkai, M. R. Duchen, Separating NADH and NADPH fluorescence in live cells and tissues using FLIM. Nature Communications 5, 3936-1 to -6 (2014)
7. T. Y. Buryakina, P.-T. Su, W.J. Syu, C.A. Chang, H.-F. Fan, F.-J. Kao, Metabolism of HeLa cells revealed through autofluorescence lifetime upon infection with enterohemorrhagic eschericha coli. J. Biomed. Opt. 17(10) 101503-1 to -9
8. B. Chance, Pyridine nucleotide as an indicator of the oxygen requirements for energy-linked functions of mitochondria. Circ Res 38, I31–I38 (1976)
9. G. Deka, W.W. Wu, F.-J. Kao, In vivo wound healing diagnosis with second harmonic and fluorescence lifetime imaging. J. Biomed. Opt. 18(6), 061222-1 to -8
10. U. Gehlsen, A. Oetke, M. Szaszak, N. Koop, F. Paulsen, Andreas Gebert, G. Huettmann, P. Steven, Two-photon fluorescence lifetime imaging monitors metabolic changes during wound healing of corneal epithelial cells in vitro. Graefes Arch. Clin. Exp. Ophthalmol 250, 1293-1302 (2012)
11. S. Kalinina, V. Shcheslavskiy, W. Becker, J. Breymayer, P. Schäfer, A. Rück, Correlative NAD(P)H-FLIM and oxygen sensing-PLIM for metabolic mapping. J. Biophotonics 9(8):800-811 (2016)
12. K. König, A. Uchugonova, E. Gorjup, Multiphoton Fluorescence Lifetime Imaging of 3D-Stem Cell Spheroids During Differentiation. Microsc. Res. Techn. 74, 9-17(2011)
13. J.R. Lakowicz, H. Szmacinski, K. Nowaczyk, M.L. Johnson, Fluorescence lifetime imaging of free and protein-bound NADH, PNAS **89**, 1271-1275 (1992)
14. A. V. Meleshina, V. V. Dudenkova, M. V. Shirmanova, V. I. Shcheslavskiy, W. Becker, A. S. Bystrova, E. I. CherkasovaE. V. Zagaynova, Probing metabolic states of differentiating stem cells usingtwo-photon FLIM. Scientific Reports 6:21853 (2016)
15. M.V. Shirmanova, V.I. Shcheslavskiy, M.M. Lukina, W. Becker, E.V. Zagaynova, Exploring tumor metabolism with time-resolved fluorescence methods: from single cells to a whole tumor. In: V. Tuchin, J. Popp, V. Zakharov, Multimodal Optical Diagnostics of Cancer. Springer (2020)
16. R.J. Paul, H. Schneckenburger, Oxygen concentration and the oxidation-reduction state of yeast: Determination of free/bound NADH and flavins by time-resolved spectroscopy, Naturwissenschaften **83**, 32-35 (1996)
17. A. Heikal, Intracellular coenzymes as natural biomarkers for metabolic activities and mitochondrial anomalies. Biomark. Med. 4(2), 241–263 (2010)
18. M. Szaszak, P. Steven, K. Shima, R. Orzekowsky-Schröder, Gereon Hüttmann, I.R. König, W. Solbach, J. Rupp, Fluorescence Lifetime Imaging Unravels C. trachomatis Metabolism and Its Crosstalk with the Host Cell. PLOS Pathogens 7, e1002108-1 to 12 (2011)
19. M. C. Skala, K. M. Riching, D. K. Bird, A. Dendron-Fitzpatrick, J. Eickhoff, K. W. Eliceiri, P. J. Keely, N. Ramanujam, In vivo multiphoton fluorescence lifetime imaging of protein-bound and free nicotinamide adenine dinucleotide in normal and precancerous epithelia. J. Biomed. Opt. 12 02401-1 to 10 (2007)
20. M. C. Skala, K. M. Riching, A. Gendron-Fitzpatrick, J. Eickhoff, K. W. Eliceiri, J. G. White, N. Ramanujam, In vivo multiphoton microscopy of NADH and FAD redox states, fluorescence lifetimes, and cellular morphology in precancerous epithelia, PNAS 104, 19494-19499 (2007)
21. R. Suarez-Ibarrola, L. Braun, P. Fabian Pohlmann, W. Becker, A. Bergmann, C. Gratzke, A. Miernik, K. Wilhelm, Metabolic Imaging of Urothelial Carcinoma by Simultaneous Autofluorescence Lifetime Imaging (FLIM) of NAD(P)H and FAD. Clinical Genitourinary Cancer (2020)
22. A. J. Walsh, R. S. Cook, H. C. Manning, D. J. Hicks, A. Lafontant, C. L. Arteaga, M. C. Skala, Optical Metabolic Imaging Identifies Glycolytic Levels, Subtypes, and Early-Treatment Response in Breast Cancer. Cancer Res. 73, 6164-6174 (2013)
23. A. J. Walsh, R. S. Cook, M. E. Sanders, L. Aurisicchio, G. Ciliberto, C. L. Arteaga, M. C. Skala, Quantitative Optical Imaging of Primary Tumor Organoid Metabolism Predicts Drug Response in Breast Cancer. Cancer Res 74, OF1-OF11 (2014)
24. Q. Yu, A. A. Heikal, Two-photon autofluorescence dynamics imaging reveals sensitivity of intracellular NADH concentration and conformation to cell physiology at the single-cell level. J. Photochem. Photobiol. B 95, 46-57 (2009)

Contact:
Wolfgang Becker, Becker & Hickl GmbH, Berlin, Germany. Email: becker@becker-hickl.com